Kinetics and Catalysis, Vol. 42, No. 1, 2001, pp. 55–63. Translated from Kinetika i Kataliz, Vol. 42, No. 1, 2001, pp. 62–71.

# Mechanisms of Reactions of $H_2O$ and $NH_3$ Molecules with $(\equiv Si–O)_3Si^•$ and $(\equiv Si–O)_3Si–O^•$ Radicals on the Silica Surface

**V. A. Radtsig and S. N. Kozlov**
*Semenov Institute of Chemical Physics, Russian Academy of Sciences, Moscow, 117977 Russia*

Received January 11, 2000

**Abstract**—Spin traps, which are diamagnetic centers $(\equiv SiO)_2Si$, are used to register low-molecular radicals $^•OH$, $^•NH_2$, and H formed by the reactions of $H_2O$ and $NH_3$ molecules with the radicals $(\equiv Si–O)_3Si^•$ and $(\equiv Si–O)_3Si–O^•$ stabilized on the silica surface. The experimental data and the results of quantum-chemical calculations for model systems are used to determine the mechanism and thermochemical characteristics of these reactions. A new paramagnetic center $(\equiv Si–O)_2Si^•NH_2$ was identified on the silica surface, and its radiospectroscopic characteristics are determined.

## INTRODUCTION

Homogeneous–heterogeneous reactions comprise a wide range of phenomena where active species leave solid surfaces. However, the data on the mechanisms of these reactions are scant. This is largely due to the absence of reliable data on the nature of active sites on solid surfaces that participate in these reactions. A rare exception is silica. For this system, the structures of the main types of paramagnetic and diamagnetic defects are determined, and their properties are studied, which make it possible to control of the processes of their formation and transformation [1–3]. Based on the study of the chemical properties of various surface defects, methods are developed that enable transforming defects of one type into others [2, 3]. Using these methods, one can obtain samples with desired point defects stabilized on the surface. This article is devoted to the experimental and quantum-chemical data on the mechanisms of the reactions of $H_2O$ and $NH_3$ molecules with paramagnetic defects stabilized on the silica surface.

The results of these studies can be of interest to environmental science. Huge masses of sand in deserts are in constant motion. (The main component of sand is silica.) Due to the friction of sand particles, various defects are formed and stabilized on their surfaces. Similar processes occur when silica powder is treated in special mechanical activators [1–4]. The cited defects are $(\equiv Si–O)_3Si^•$ and $(\equiv Si–O)_3Si–O^•$, which are the products of the homolytic cleavage of siloxane bonds. The latter can react with the molecules of a surrounding gas atmosphere, including water molecules.

When studying the reactions of paramagnetic defects with saturated molecules, such as $H_2O$ and $NH_3$, low-molecular radicals can be formed. One of the methods for determining the structures of these low-molecular radicals is the use of spin traps when some groups play the role of the acceptors of free radicals formed. In this study, we used samples of reactive silica (RS) [5]. On the surface of such a sample, diamagnetic defects ($(\equiv Si–O)_2Si\colon$ (X)) are present together with paramagnetic ones [2, 3]. Diamagnetic defects are usually moderately active toward saturated molecules, but they are efficient traps for low-molecular spin radicals. Therefore, if mobile free radicals ($R^•$) are formed in the system during a chemical process, they can be trapped by these groups to form paramagnetic complexes $(XR)^•$. Direct spectral methods (ESR, IR spectroscopy, and optical methods) can be used to register such complexes. The elucidation of their structures may provide data on the nature of radical $R^•$.

## EXPERIMENTAL

Experiments were carried out with powdered high-dispersity Aerosil A-300 with an initial specific surface area of ~300 $m^2/g$. The method of silica surface activation resulting in a substantial increase in its chemical activity (the formation of RS) was proposed by Morterra and Low and described in detail in [2, 5, 6]. As a result of high-temperature treatment (RS preparation includes the stage of high-temperature treatment at 1200 K), the value of the Aerosil specific surface area decreased to 100–150 $m^2/g$. Two types of defects are stabilized on the surface of activated powder: paramagnetic radicals $(\equiv Si–O)_3Si^•$ with a concentration of $\sim 1 \times 10^{12}$ or $\sim 10^{17}$ $cm^{-2}$ per sample and diamagnetic centers $(\equiv Si–O)_2Si\colon$ with two-coordinated silicon atoms. The concentration of diamagnetic centers is more than an order of magnitude higher than the concentration of paramagnetic centers. We denote this system as $((\equiv\text{Si–O})_3\text{Si}^\bullet, (\equiv\text{Si–O})_2\text{Si:})$. Another system is $((\equiv\text{Si–O})_3\text{Si–O}^\bullet, (\equiv\text{Si–O})_2\text{Si:})$. To obtain it, the $((\equiv\text{Si–O})_3\text{Si}^\bullet, (\equiv\text{Si–O})_2\text{Si:})$ sample was treated by $N_2O$ molecules at room temperature. The $N_2O$ molecules undergo addition to silyl radicals:[1]

$$(\equiv\text{Si–O})_3\text{Si}^\bullet + \text{N}_2\text{O} \longrightarrow (\equiv\text{Si–O})_3\text{Si–N=N–O}^\bullet$$

When heated to a temperature higher than 373 K, the complex decomposes to form an oxy radical and a gaseous nitrogen molecule:

$$(\equiv\text{Si–O})_3\text{Si–N=N–O}^\bullet \longrightarrow (\equiv\text{Si–O})_3\text{Si–O}^\bullet + \text{N}_2.$$

This treatment does not concern centers involving two-coordinated silicon atoms. Thus, we obtained the sample $((\equiv\text{Si–O})_3\text{Si–O}^\bullet, (\equiv\text{Si–O})_2\text{Si:})$, on the surface of which oxy radicals and diamagnetic silylene groups are stabilized.

All experiments were carried out in a high vacuum or under the conditions of controlled atmosphere. The pressures of $H_2O$ and $NH_3$ vapors in the system were measured using the Pirani gauge. At room temperature, vapors are adsorbed on the walls of a vacuum system and especially on the powder surface. This prevented us from obtaining quantitative data on the rate constants of the processes under study.

The ESR spectra of samples were recorded at 300 or 77 K using an EPR-20 spectrometer from the Institute of Chemical Physics working in the X-range. Due to the specific features of the electronic structure, the registration of the $(\equiv\text{Si–O})_3\text{Si–O}^\bullet$ radicals by ESR under ordinary conditions is difficult [8]. A more convenient method is to control the concentration of these radicals in the sample using the luminescence method [9, 10]. Oxy radicals have a band with an absorbance maximum near 4.7 eV. The absorption of a light quantum is accompanied by red luminescence near 2.0 eV. This enables the control of the oxy radical concentration in the sample by monitoring a change in the level of chemiluminescence.

Quantum-chemical calculations were carried out using the Gaussian-94 program package [11]. We used molecular models of surface defects of silica. It has been shown before [3, 12] that low-molecular compounds $F_2SiXY$ and $F_3SiX$ in which the ≡Si–O group(s) is (are) replaced by a fluorine atom are very close in their physicochemical characteristics to the surface sites of silica $(\equiv\text{Si–O})_2\text{SiXY}$ or $(\equiv\text{Si–O})_3\text{SiX}$ (where X and Y are low-molecular substituents). The structure optimization was performed using density functional theory (DFT) within the gradient approximation (B3LYP/6-311G**) [13, 14]. For all optimized structures, we calculated their vibrational spectra. Transition states were characterized by a single negative eigenvalue of the Hessian matrix. The values of reaction enthalpies were determined at 0 K from the equation $\Delta H(0\text{K}) = \Delta E(0\text{K}) + \Delta(ZPE)$, where $\Delta E(0\text{ K})$ is the difference between the total energies of initial reactants and final products and $\Delta(ZPE)$ is the difference between their zero-point energies. The corresponding results are summarized in Tables 1 and 2. The values of enthalpies $\Delta H(0\text{K})$ for two reactions calculated by this method are given below (for these reactions, experimental values are available and shown in parentheses [15]):

$$\text{HOH} \longrightarrow {}^\bullet\text{OH} + {}^\bullet\text{H} + 111.6\ (119.2)\ \text{kcal/mol},$$

$$\text{NH}_3 \longrightarrow {}^\bullet\text{NH}_2 + {}^\bullet\text{H} + 102.5\ (108.2)\ \text{kcal/mol}.$$

## RESULTS AND DISCUSSION

**System $((\equiv\text{Si–O})_3\text{Si–O}^\bullet, (\equiv\text{Si–O})_2\text{Si:}) + H_2O$.** The sample contact with water vapors at 300 K was accompanied by the disappearance of photoluminescence from oxy radicals (the vapor pressure was at most $10^{-1}$ torr). This points to their decay when they interacted with water. New paramagnetic centers were detected in the reaction products by the ESR method. Their ESR spectrum is shown in Fig. 1. An analogous ESR signal belonging to the $(\equiv\text{Si–O})_2\text{Si}^\bullet\text{OH}$ radicals was first observed in [16]. This signal is a superposition of the ESR spectra of the radicals $(\equiv\text{Si–O})_2{}^{28,30}\text{Si}^\bullet\text{–OH}$ (95.3%) (Fig. 1a) and $(\equiv\text{Si–O})_2{}^{29}\text{Si}^\bullet\text{–OH}$ (4.7%) (Fig. 1b). Two lines (~5% of the central signal intensity) (Fig. 1b) belong to the radicals containing a $^{29}$Si isotope ($I = 1/2$, the natural concentration is 4.7%) for which $a_{\text{iso}}(^{29}\text{Si}) = -413 \pm 1$, $b_1 \cong b_2 = 18.7 \pm 0.5$, and $b_3 = -37.4 \pm 1$ G [17]. The central line belongs to the radicals containing $^{28}$Si and $^{30}$Si isotopes ($I = 0$, the overall natural concentration is 95.3%) (Fig. 1a). The shape of the ESR spectrum of this radical reversibly changes with the temperature of spectra recording. At 77 K, the hyperfine structure due to a proton is more pronounced in the central part of the spectrum.

The $(\equiv\text{Si–O})_2\text{Si}^\bullet\text{OH}$ radicals were registered as the products of the addition of the ${}^\bullet\text{OH}$ radicals to diamagnetic silylene centers [18]. In that study, ${}^\bullet\text{OH}$ is the product of the thermal decomposition of the radical $(\equiv\text{Si–O})_2\text{Si}(\text{C}_2\text{H}_5)(\text{O–O}^\bullet)$.

Thus, the experimental data suggest that the interaction of a water molecule with silyl oxy radicals occurs as follows:

$$(\equiv\text{Si–O})_3\text{Si–O}^\bullet + \text{H}_2\text{O} \longrightarrow (\equiv\text{Si–O})_3\text{Si–O–H} + {}^\bullet\text{OH}, \tag{I}$$

---

[1] Earlier it was suggested [7] that the complex formed has a different structure: $(\equiv\text{Si–O})_3\text{Si–O–N=N}^\bullet$. This problem will be discussed in a separate paper.

**Table 1.** Results of the DFT calculations of total energies ($E$(0 K)) and zero-point energies ($ZPE$) of the systems under study: molecules, radicals, complexes, and transition states (TS)*

| Compound | $-E$(0 K), at. u. | $ZPE$, kcal/mol | $\langle S^2 \rangle$ |
|---|---|---|---|
| 1. $H^\bullet$ | 0.50216 | 0 | 0.750 |
| 2. $^\bullet OH$ | 75.75453 | 5.3 | 0.752 |
| 3. HOH | 76.44745 | 13.4 | – |
| 4. $^\bullet NH_2$ | 55.89510 | 11.85 | 0.753 |
| 5. $NH_3$ | 56.57604 | 21.5 | – |
| 6. $F_2Si$ | 489.34462 | 2.9 | – |
| 7. $F_3Si^\bullet$ | 589.25327 | 5.2 | 0.751 |
| 8. $F_3SiH$ | 589.92004 | 11.3 | – |
| 9. $F_3SiO^\bullet$ | 664.51516 | 7.3 | 0.752 |
| 10. $F_3SiOH$ | 665.22070 | 14.6 | – |
| 11. $F_2Si^\bullet OH$ | 565.21917 | 12.1 | 0.751 |
| 12. $F_2Si^\bullet NH_2$ | 545.33421 | 19.5 | 0.752 |
| 13. $F_3SiNH_2$ | 645.33595 | 22.1 | – |
| 14. $(F_3Si^\bullet \ldots H_2O)$ (complex) | 665.71777 | 20.4 | 0.751 |
| 15. $(F_3Si^\bullet \ldots NH_3)$ (complex) | 645.85468 | 29.1 | 0.751 |
| 16. $F_3Si^\bullet \ldots HOH \longrightarrow F_3SiOH + H$ (TS) | 665.68317 | 15.3 | 0.754 |
| 17. $F_3Si^\bullet \ldots NH_3 \longrightarrow F_3SiNH_2 + H$ (TS) | 645.81271 | 24.5 | 0.756 |
| 18. $F_3Si^\bullet \ldots NH_3 \longrightarrow F_3SiH + {}^\bullet NH_2$ (TS) | 645.81000 | 23.4 | 0.756 |

* For free radicals, the value $\langle S^2 \rangle$ is the average value of the square of the spin operator for the system. For purely doublet states, this value equals 0.75.

$$(\equiv Si–O)_2Si\colon + {}^\bullet OH \longrightarrow (\equiv Si–O)_2Si^\bullet(OH). \qquad (II)$$

Reaction (I) is exothermic: the strength of the O–H bond in the ≡Si–O–H group is higher than in a water molecule [19, 20]. The results of quantum-chemical calculations (Table 2, reaction 1) suggest the same.

It was noted in [21] that the $(\equiv Si–O)_3Si–O^\bullet$ radicals are more active in the reactions of H abstraction than $^\bullet OH$ radicals. We failed to find any data on the activation energy of the reaction $^\bullet OD + HOH \longrightarrow HOD + {}^\bullet OH$. Supposedly, it is within a range of 5–10 kcal/mol. For reaction (I), it is even lower.

Table 2 (reaction 9) specifies a value for the enthalpy of hydroxyl radical addition to a diamagnetic center containing a two-coordinated silicon atom.

**System $((\equiv Si–O)_3Si–O^\bullet$, $(\equiv Si–O)_2Si\colon) + NH_3$.** The contact of the sample with ammonia vapors at 300 K (the vapor pressure was at most $10^{-1}$ torr) was also accompanied by the decay of oxy radicals (according to photoluminescence data). The formation of new paramagnetic centers was registered by the ESR method (Fig. 2). We assign this spectrum to the radicals $(\equiv Si–O)_2{}^{28,30}Si^\bullet NH_2$ (95.3%) (Fig. 2a) and $(\equiv Si–O)_2{}^{29}Si^\bullet NH_2$ (4.7%) (Fig. 2b). An unpaired electron in this radical is localized at the silicon atom. This follows from the characteristic value of the constant of hyperfine interaction between the unpaired electron and the nucleus of a silicon atom in the $(\equiv Si–O)_2{}^{29}Si^\bullet NH_2$ radical. Two lines belong to these radicals located at the wings of the spectrum ($a_{iso}(^{29}Si) = -377 \pm 1$, $b_1 \cong b_2 = 18.6 \pm 0.5$, and $b_3 = -37.2 \pm 1$ G; signs were chosen according to the results of quantum-chemical calculations (*vide infra*)). The intensity of these lines is ~5% of the intensity of the main spectrum.

The triplet structure of the ESR spectra of the radicals $(\equiv Si–O)_2{}^{29}Si^\bullet NH_2$ and $(\equiv Si–O)_2{}^{28}Si^\bullet NH_2$ with a ratio between the component intensities of 1 : 1 : 1 is due to the $^{14}N$ atom ($I = 1$). The form of the central component of the triplet ($M_I = 0$) of the $(\equiv Si–O)_2{}^{28}Si^\bullet NH_2$ radical is determined by the anisotropy of the $g$-tensor, the main values of which are $g_1 = 2.0018 \pm 0.0001$, $g_2 =$

**Table 2.** Results of the DFT calculations of the reaction enthalpies of some reactions with silicon-containing free radicals and $H_2O$ and $NH_3$ molecules

| Reaction | $\Delta H$(0 K), kcal/mol |
|---|---|
| 1. $F_3Si{-}O^{\bullet} + H_2O \longrightarrow F_3Si{-}O{-}H + {}^{\bullet}OH$ | −8.7 |
| 2. $F_3Si{-}O^{\bullet} + NH_3 \longrightarrow F_3Si{-}O{-}H + {}^{\bullet}NH_2$ | −17.7 |
| 3. $F_3Si^{\bullet} + H_2O \longrightarrow F_3Si{-}O{-}H + {}^{\bullet}H$ | −9.9 |
| 4. $F_3Si^{\bullet} + NH_3 \longrightarrow F_3Si{-}NH_2 + H$ | −10.2 |
| 5. $F_3Si^{\bullet} + H_2O \longrightarrow F_3Si{-}H + {}^{\bullet}OH$ | 14.3 |
| 6. $F_3Si^{\bullet} + NH_3 \longrightarrow F_3Si{-}H + {}^{\bullet}NH_2$ | 5.3 |
| 7. $F_3Si{-}OH \longrightarrow F_3Si^{\bullet} + {}^{\bullet}OH$ | 129.5 |
| 8. $F_3Si{-}NH_2 \longrightarrow F_3Si^{\bullet} + {}^{\bullet}NH_2$ | 112.7 |
| 9. $F_2Si: + {}^{\bullet}OH \longrightarrow F_2Si^{\bullet}OH$ | −71.5 |
| 10. $F_2Si: + {}^{\bullet}NH_2 \longrightarrow F_2Si^{\bullet}NH_2$ | −54.5 |
| 11. $F_2Si: + H \longrightarrow F_2Si^{\bullet}H$ | −40.4 |
| 12. $(F_3Si^{\bullet}\ldots H_2O)$ (complex) | −8.9 |
| 13. $(F_3Si^{\bullet}\ldots NH_3)$ (complex) | −13.5 |

$2.0011 \pm 0.0001$, $g_3 = 2.0002 \pm 0.0001$, and $g_{iso} = 2.0010$ at 300 K. These are typical values for the silyl radicals containing electronegative substituents [3, 17]. The tensor of the hyperfine interaction of an unpaired electron with the $^{14}N$ nucleus at 300 K has the following main values: $a_1 = 15.4 \pm 0.2$, $a_2 = 10.9 \pm 0.2$, $a_3 = 12.1 \pm 0.2$, and $a_{iso} = 12.8 \pm 0.2$ G (the components are renumbered in the same order as the components of the $g$-tensor). The hyperfine interaction of an unpaired electron with protons in the ESR spectrum of this radical at 300 K does not reveal itself in the form of a resolved hyperfine structure.

If the spectrum was recorded at 77 K, the form of the ESR signal reversibly changed. This fact points to frozen internal rotations in the radical.

Below we report the calculations of radiospectroscopic characteristics for paramagnetic centers of this type using the $F_2Si^{\bullet}NH_2$ radical as an example. This radical modeled the surface center $(\equiv Si{-}O)_2Si^{\bullet}NH_2$. Figure 3 (structure **I**) shows the optimized structure of this radical. Table 3 lists the calculated tensors of hyperfine interaction. The values of constants are determined from the calculated values of the contact Fermi and dipole–dipole interactions between unpaired electrons and the magnetic momentum of the corresponding nucleus.

According to calculations, the height of the activation barrier for the $NH_2$ group rotation around the Si–N bond in the $F_2Si^{\bullet}NH_2$ radical is at most 2 kcal/mol. During $NH_2$ group rotation, the value of the constant of hyperfine interaction with a silicon atom changes by only several percent, although a change in the value of the isotropic constant of hyperfine interaction with a nitrogen nucleus is more pronounced: it can double. Therefore, the value of the $a_{iso}(^{14}N)$ constant in Table 3 should increase if thermal motion is taken into account. On the other hand, shifts should lead to the averaging of the anisotropic component of the tensor of hyperfine interaction of the unpaired electron with a nitrogen nucleus. Thus, the values of hyperfine interaction constants obtained in the experiment for the surface defect and calculated for the $F_2Si^{\bullet}NH_2$ radical agree acceptably with each other. This is further evidence for the correctness of the structure proposed for the center structure. The calculated vibration frequencies for the $NH_2$ group in the radical are 1583 $cm^{-1}$ (deformational vibration) and 3566 and 3660 $cm^{-1}$ (symmetrical and asymmetrical stretching vibrations). In the last section of this article, we will explain the empirical correction of these values.

Proceeding from the structure of radicals formed and the method of their generation, we can assume that they are formed via the same scheme as the $(\equiv Si{-}O)_2Si^{\bullet}OH$ radicals in the course of the interaction of oxysilyl radicals with water molecules. First, an oxy radical abstracts a hydrogen atom from an ammonia molecule:

$$(\equiv Si{-}O)_3Si{-}O^{\bullet} + NH_3 \longrightarrow (\equiv Si{-}O)_3Si{-}O{-}H + {}^{\bullet}NH_2. \qquad \text{(III)}$$

Then, the low-molecular radical formed in this reaction is added to the diamagnetic silylene center:

$$(\equiv Si{-}O)_2Si\!: + {}^{\bullet}NH_2 \longrightarrow (\equiv Si{-}O)_2Si^{\bullet}NH_2. \qquad \text{(IV)}$$

The enthalpy of reaction (III) is 11 kcal/mol higher than that of reaction (I) (the difference between the strengths of the O–H and N–H bonds in the molecules of water and ammonia). The calculation led us to a value of ~9 kcal/mol (see reactions 1 and 2 in Table 2).

Table 2 (reaction 10) also contains the value of the enthalpy for the reaction of ${}^{\bullet}NH_2$ radical addition to the diamagnetic center $F_2Si\!:$. As was expected, this value is noticeably lower than in the case of a hydroxysilyl radical (the difference is 17 kcal/mol according to the calculation).

According to [22], the activation energy of the reaction

$$^{\bullet}OH + NH_3 \longrightarrow H{-}O{-}H + {}^{\bullet}NH_2$$

is ~3 kcal/mol. Taking into account a higher reactivity of silyl oxy radicals (see above), we assume that the height of the activation barrier for reaction (III) is still lower. Under our conditions, the rate of this reaction is limited by ammonia diffusion to surface centers through silica powder.

**System ($(\equiv$Si–O$)_3$Si$^\bullet$, $(\equiv$Si–O$)_2$Si:) + $H_2O$.** The contact of the sample with water vapors at 420 K was accompanied by the decay of silyl radicals and by the formation of new paramagnetic centers (the maximal vapor pressure was $10^{-1}$ torr). Figure 4 shows their ESR spectrum. It belongs to the radicals $(\equiv\text{Si–O})_2{}^{28,30}\text{Si}^\bullet\text{–H}$ (95.3%) (Fig. 4a) and $(\equiv\text{Si–O})_2{}^{29}\text{Si}^\bullet\text{–H}$ (4.7%) (Fig. 4b) [23]. The hyperfine structure of the ESR spectra of these radicals is stipulated by the interaction of an unpaired electron with a proton ($a(^1\text{H}) \approx 81$ G) and the α-Si atom ($a_\perp(^{29}\text{Si}) = -289 \pm 1$, $a_\parallel(^{29}\text{Si}) = -355 \pm 1$, $a_\text{iso}(^{29}\text{Si}) = -311 \pm 1$, $b_1(^{29}\text{Si}) \cong b_2(^{29}\text{Si}) = 22 \pm 1$, and $b_3(^{29}\text{Si}) = -44 \pm 1$ G).

Figure 5 illustrates the dependence of the relative concentrations of the $(\equiv\text{Si–O})_3\text{Si}^\bullet$ radicals and the $(\equiv\text{Si–O})_2\text{Si}^\bullet\text{–H}$ radicals during this reaction. This dependence is linear. The overall concentration of paramagnetic centers remains virtually constant.

The appearance of the $(\equiv\text{Si–O})_2\text{Si}^\bullet\text{–H}$ radicals in the system indicates that a hydrogen atom is formed in the reaction of a water molecule with a silyl radical. Then, this hydrogen atom is accepted by a diamagnetic center [24]. Thus, the process occurs as follows:

$$(\equiv\text{Si–O})_3\text{Si}^\bullet + \text{H}_2\text{O} \longrightarrow (\equiv\text{Si–O})_3\text{Si–O–H} + {}^\bullet\text{H}, \quad \text{(V)}$$

$$(\equiv\text{Si–O})_2\text{Si:} + {}^\bullet\text{H} \longrightarrow (\equiv\text{Si–O})_2\text{Si}^\bullet\text{–H}. \quad \text{(VI)}$$

The enthalpy of another reaction channel, where water reacts with a silyl radical:

$$(\equiv\text{Si–O})_3\text{Si}^\bullet + \text{H}_2\text{O} \longrightarrow (\equiv\text{Si–O})_3\text{Si–H} + {}^\bullet\text{OH} \quad \text{(VII)}$$

is much higher. Assuming that the strength of a Si–O bond in the silanol group is 125 ± 5 kcal/mol (Table 2, reaction 7) and that the Si–H bond strength is 100 ± 2 kcal/mol [19], we find that the enthalpy of reaction (V) is –7 ± 5 kcal/mol (the strength of the O–H bond in the water molecule is 119 kcal/mol [15]). The enthalpy of reaction (VII) is 18 ± 2 kcal/mol.

The results of enthalpy calculations where $\text{F}_3\text{Si}^\bullet$ plays a role of the silyl radical are summarized in Table 2 (reactions 3 and 5). Note that the experimental and calculated reaction enthalpies are in acceptable agreement.

Figure 3 shows the structure of the transition state for the reaction of the silyl radical $\text{F}_3\text{Si}^\bullet$ with a water molecule (**II**) resulting in the formation of a silanol group and a hydrogen atom. The calculated activation energy of this reaction is 7.7 kcal/mol (relative to the level of the nonreacting radical and a water molecule). We failed to localize the transition state for the second direction of the reaction. However, the activation energy of hydrogen atom abstraction from the water molecule cannot be lower than 14 kcal/mol (the reaction enthalpy). Thus, in agreement with the experimental data, the calculation shows that the main channel for the reaction is process (5) from Table 2, and its activation energy is probably 8 ± 3 kcal/mol.

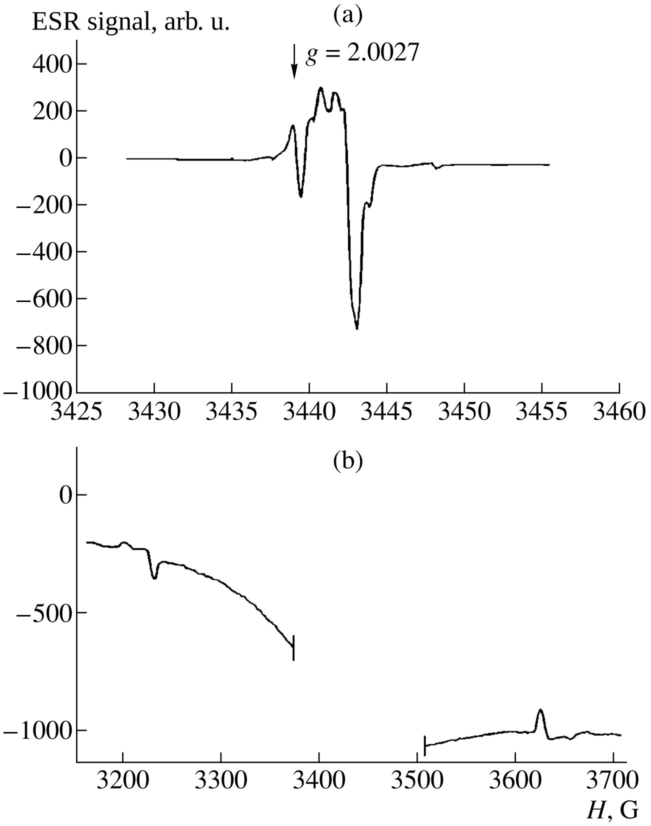

**Fig. 1.** ESR spectrum of the $(\equiv\text{Si–O})_2\text{Si}^\bullet\text{–OH}$ radicals recorded at 300 K (a singlet line with $g = 2.0027$ refers to an impurity signal): (a) $(\equiv\text{Si–O})_2{}^{28,30}\text{Si}^\bullet\text{–OH}$ and (b) $(\equiv\text{Si–O})_2{}^{29}\text{Si}^\bullet\text{–OH}$.

Table 2 (reaction 11) shows the value for the enthalpy of reaction of hydrogen addition to the $\text{F}_2\text{Si:}$ molecule. For the reaction $(\equiv\text{Si–O})_2\text{Si:} + {}^\bullet\text{H} \longrightarrow (\equiv\text{Si–O})_2\text{Si}^\bullet\text{–H}$, this value is 38 ± 2 kcal/mol [12]. This points to the closeness of the characteristics of the processes with the participation of silica surface defects and their fluorine-substituted low-molecular analogs.

**System ($(\equiv$Si–O$)_3$Si$^\bullet$, $(\equiv$Si–O$)_2$Si:) + $NH_3$.** The contact of the sample with ammonia vapors at 300 K was accompanied by the decay of silyl radicals and the

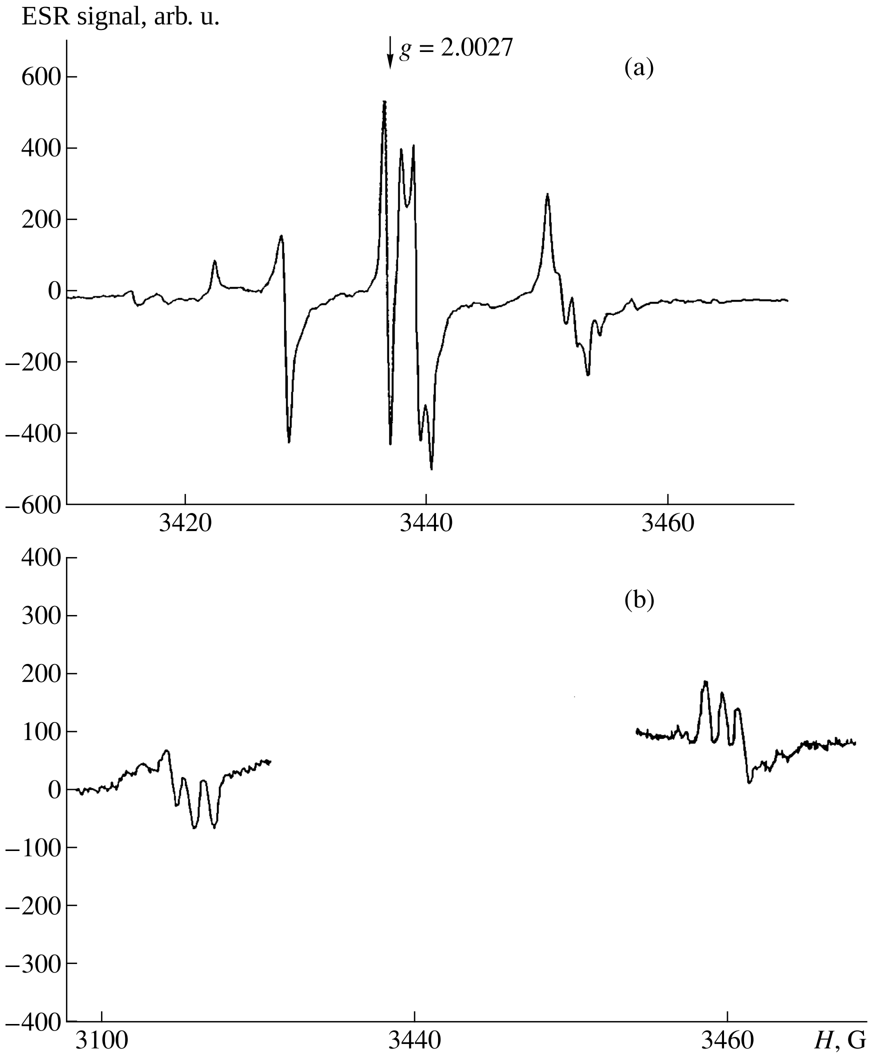

**Fig. 2.** ESR spectrum of the $(\equiv\text{Si–O})_2\text{Si}^\bullet\text{–NH}_2$ radicals recorded at 300 K (a singlet line with $g = 2.0027$ refers to an impurity signal): (a) $(\equiv\text{Si–O})_2{}^{28,30}\text{Si}^\bullet\text{–NH}_2$ and (b) $(\equiv\text{Si–O})_2{}^{29}\text{Si}^\bullet\text{–NH}_2$.

formation of new paramagnetic centers, which are the $(\equiv\text{Si–O})_2\text{Si}^\bullet\text{–H}$ radicals (the maximal vapor pressure was $10^{-1}$ torr, but substantial ammonia adsorption was observed on the silica surface). The overall concentration of paramagnetic centers remained constant with an uncertainty of 20%. Thus, the reaction of the $(\equiv\text{Si–O})_3\text{Si}^\bullet$ radicals with ammonia molecules is accompanied by the formation of atomic hydrogen as in the case of their reaction with water molecules:

$$(\equiv\text{Si–O})_3\text{Si}^\bullet + \text{NH}_3 \longrightarrow (\equiv\text{Si–O})_3\text{Si–NH}_2 + {}^\bullet\text{H}. \quad \text{(VIII)}$$

Molecular hydrogen then reacts with $(\equiv\text{Si–O})_2\text{Si}:$ by reaction (VI).

**Table 3.** Radiospectroscopic characteristics of radicals $(\equiv\text{Si–O})_2\text{Si}^\bullet\text{NH}_2$ (experiment) and $\text{F}_2\text{Si}^\bullet\text{NH}_2$ (calculation)

| Hyperfine interaction tensor | $a_{\text{iso}}$, G | | $b_1$, G | | $b_2$, G | | $b_3$, G | |
|---|---|---|---|---|---|---|---|---|
| | experiment | calculation | experiment | calculation | experiment | calculation | experiment | calculation |
| $^{29}$Si | −377 ± 1 | −391.4 | −37.2 ± 1 | −40.6 | 18.6 ± 0.5 | 20.7 | 18.6 ± 0.5 | 19.9 |
| $^{14}$N | 12.8 ± 0.3 | 8.8 | 2.6 ± 0.3 | 6.2 | −1.9 ± 0.3 | −3.2 | −0.7 ± 0.3 | −3.0 |
| $^{1}$H | $\|a_{\text{iso}}\| \le 2$ | −3.8 | – | 5.3 | – | −4.2 | – | −1.3 |

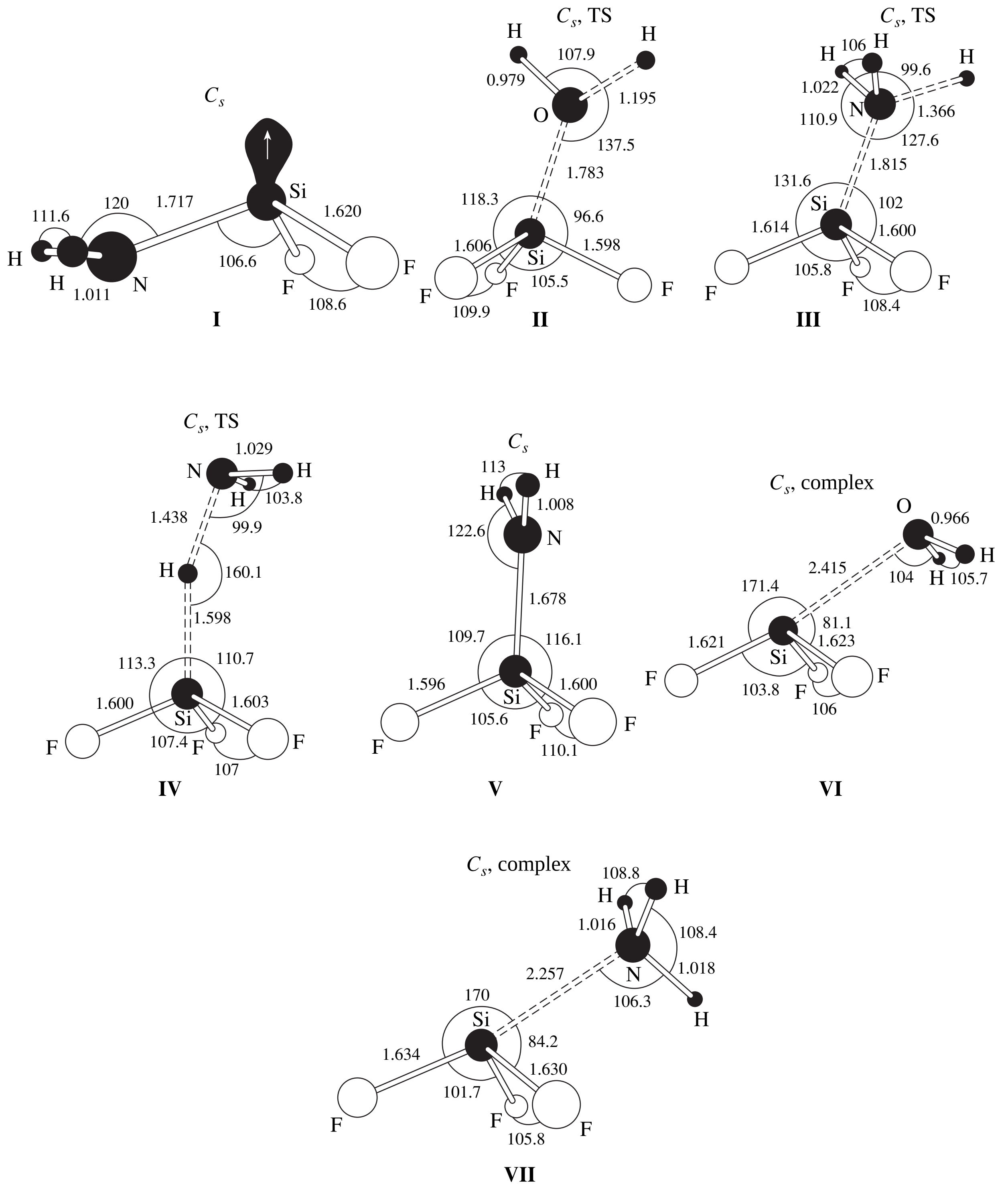

**Fig. 3.** Geometric characteristics (bond lengths in angstroms and angles in degrees) and symmetries of the systems studied: molecules radicals, complexes, and transition states (TS) (optimization at the DFT level): **I** is the $F_2\overset{\bullet}{Si}NH_2$ radical; **II** is the transition state for the reaction of the silyl radical with a water molecule to form atomic hydrogen (the imaginary frequency that characterizes the transition state is 1244i $cm^{-1}$); **III** is the transition state for the reaction of the silyl radical with an ammonia molecule to form atomic hydrogen (the imaginary frequency that characterizes the transition state is 1264i $cm^{-1}$); **IV** is the transition state for the reaction of hydrogen atom abstraction from $NH_3$ by the silyl radical (the imaginary frequency that characterizes the transition state is 1045i $cm^{-1}$); **V** is the $F_2Si–NH_2$ molecule; **VI** is the complex of the silyl radical with $H_2O$; and **VII** is the complex of the silyl radical with $NH_3$.

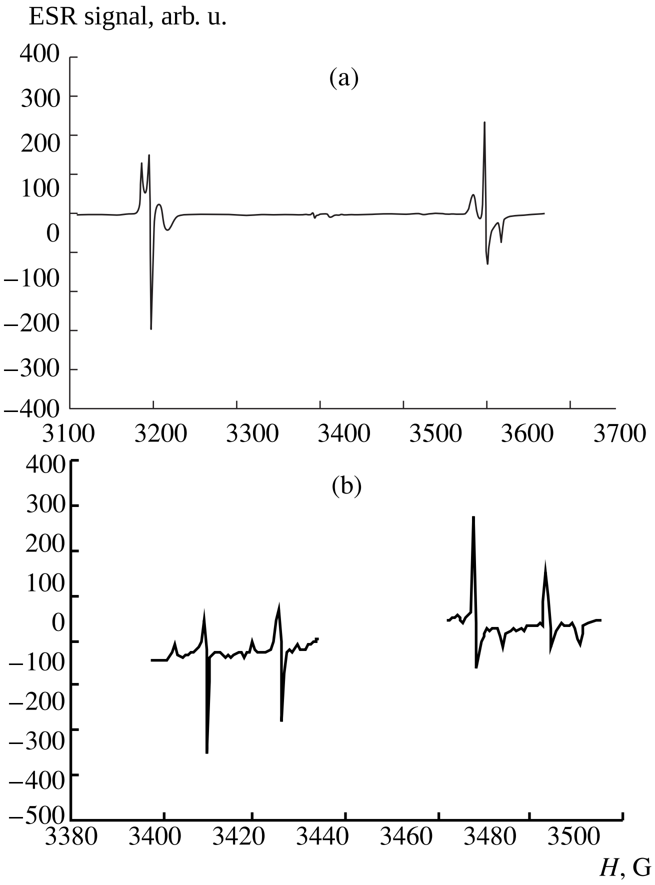

**Fig. 4.** ESR spectrum of the $(\equiv\text{Si–O})_2\text{Si}^{\bullet}\text{–H}$ radicals recorded at 300 K: (a) $(\equiv\text{Si–O})_2{}^{28,30}\text{Si}^{\bullet}\text{–H}$ and (b) $(\equiv\text{Si–O})_2{}^{29}\text{Si}^{\bullet}\text{–H}$.

The results of calculations giving an insight into some thermochemical characteristics of the "silyl radical + ammonia" system are presented in Table 2 (reactions 4, 6, and 8). According to the calculations, the strength of the Si–N bond is 17 kcal/mol lower than the strength of the Si–O bond (Table 2, reactions 7 and 8). In an ammonia molecule, the strength of the N–H bond is 11 kcal/mol lower than the strength of the O–H bond in a water molecule. Reaction (VIII) with the formation of a hydrogen atom is exothermic in the case of both ammonia and water. The reaction of hydrogen abstraction is endothermic in both systems.

Figure 3 shows the structures of transition states for two channels of the reaction of the $F_3Si^{\bullet}$ radical with ammonia resulting in the formation of the hydrogen atom (structure **III**) and the $^{\bullet}NH_2$ radical (structure **IV**). The activation energies of the first and second reactions are 8.2 and 8.8 kcal/mol, respectively. That is, the results of quantum-chemical calculations show that the formation of atomic hydrogen is probably the main reaction channel in this system as well.

Figure 3 shows the optimized structure (**V**) of the reaction product $F_3Si–NH_2$. In this molecule, N is slightly shifted relative to the (H, Si, H) plane. The value of the dihedral angle HNHSi is 165°. In an ammonia molecule, the value of the dihedral angle HNHH is 113.3° (according to DFT calculation). Thus, the replacement of the hydrogen atom by the $SiF_3$ group results in the flattening of the nitrogen coordination sphere.

The frequencies of $NH_2$ group vibrations in the $F_3Si–NH_2$ molecule are 1593 $cm^{-1}$ (deformational) and 3610 and 3700 $cm^{-1}$ (symmetric and asymmetric stretching vibrations). The transfer of the radical to a saturated molecule resulted in a small increase in the frequencies; that is, the corresponding chemical bonds became somewhat stronger.

In the calculations, the frequencies of stretching vibrations with the participation of a light hydrogen atom are overestimated. This is because the harmonic frequency of vibration is determined in these calculations, and vibration anharmonicity is especially pronounced in this case. Also, some inaccuracy in the calculation of the force field makes its contribution. An empirical method of scaling factors, according to which the calculated value is multiplied by the ratio of experimental versus calculated frequencies for similar structures, makes it possible to correct the calculated values. The vibration frequencies of the $NH_2$ group in the composition of the $(\equiv\text{Si–O})_3\text{Si–NH}_2$ surface fragment were determined in experiments. These are 1550, 3443, and 3530 $cm^{-1}$ [25, 26]. Using the values measured for $(\equiv\text{Si–O})_3\text{Si–NH}_2$ and experimentally determined values for $F_3Si–NH_2$ as scaling factors, we corrected the values of vibrational frequencies for the $NH_2$ group in the $F_2Si^{\bullet}NH_2$ radical: 1583 → 1540, 3566 → 3401, and 3660 → 3492 $cm^{-1}$. Here, we assumed that the frequencies of $NH_2$ group vibrations in the $(\equiv\text{Si–O})_2\text{Si}^{\bullet}\text{NH}_2$ radical have close values.

According to quantum-chemical calculations, silyl radicals form rather strong intramolecular complexes with the $H_2O$ and $NH_3$ molecules. Figure 3 (**VI** and **VII**) shows their structures. The heats of their formation are listed in Table 2 (reactions 12 and 13). We may assume that the activation energy for the reactions that form these complexes is barely higher than 1–2 kcal/mol. Note that the strength of the ammonia complex is very high.

Thus, the interaction of water and ammonia molecules with paramagnetic centers on the silica surface is accompanied by the formation of chemically active low-molecular free radicals. If these radicals escape to the gas phase, they are capable of initiating chemical processes in the surrounding medium. A specific feature of the reaction between the silyl radical and $H_2O$ and $NH_3$ molecules is the formation of atomic hydrogen. These processes are unusual for carbon-centered free radicals.

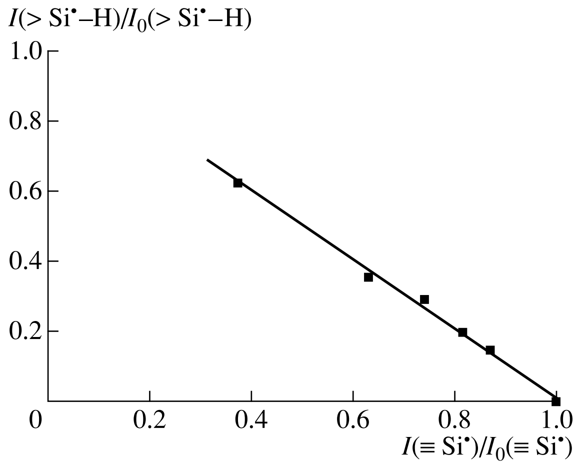

**Fig. 5.** Relations between the concentrations of the centers $(\equiv Si–O)_3Si^\bullet$ and $(\equiv Si–O)_2Si^\bullet–H$ in the reaction of silyl radicals with the $H_2O$ molecules (ESR measurements).

## ACKNOWLEDGMENTS

This work was supported by the Russian Foundation for Basic Research (project nos. 97-03-32384 and 98-03-32258). Quantum-chemical calculations were carried out using the Gaussian 94 program [11] at the Institute of Organic Chemistry (Russian Foundation for Basic Research, project no. 98-07-90290).

## REFERENCES

1. Hochstrasser, G. and Antonini, I., *Surf. Sci.*, 1972, vol. 31, p. 644.
2. Radtsig, V.A., *Khim. Fiz.*, 1995, vol. 14, no. 8, p. 125.
3. Radtsig, V.A., *Kinet. Katal.*, 1999, vol. 40, no. 5, p. 764.
4. Butyagin, P.Yu., Berlin, A.A., and Kalmanson, A.E., *Vysokomol. Soedin.*, 1959, vol. 1, no. 6, p. 865.
5. Morterra, C. and Low, M.J.D., *Ann. N.-Y. Acad. Sci.*, 1973, vol. 220, p. 133.
6. Morterra, C. and Low, M.J.D., *J. Phys. Chem.*, 1969, vol. 73, no. 2, p. 321.
7. Radtsig, V.A., *Kinet. Katal.*, 1979, vol. 20, no. 2, p. 448.
8. Radtsig, V.A. and Bystrikov, A.V., *Kinet. Katal.*, 1978, vol. 19, no. 3, p. 713.
9. Streletskii, A.N., Pakovich, A.B., Aristov, Yu.I., *et al.*, *Khim. Fiz.*, 1982, vol. 1, p. 938.
10. Skuja, L.N., Streletsky, A.N., and Pakovich, A.B., *Solid State Commun.*, 1984, vol. 50, no. 12, p. 1069.
11. Frisch, M.J., Trucks, G.W., Schlegel, H.B., *et al.*, *Gaussian 94, Revision D. 1*, Pittsburgh, PA: Gaussian Inc., 1995.
12. Radtsig, V.A., *Kinet. Katal.*, 1996, vol. 37, no. 2, p. 310.
13. Becke, A.D., *J. Chem. Phys.*, 1993, vol. 98, no. 7, p. 5648.
14. Lee, C., Yang, W., and Parr, R.G., *Phys. Rev. B*, 1988, vol. 37, no. 2, p. 785.
15. Chase, M.W., Davies, C.A., Downey, J.R., and Frurip, D.J., *J. Phys. Chem. Ref. Data.*, 1985, suppl. 1, vol. 14, p. 1.
16. Bobyshev, A.A. and Radtsig, V.A., *Kinet. Katal.*, 1988, vol. 29, no. 3, p. 638.
17. Radtsig, V.A., *Khim. Fiz.*, 2000, vol. 19, no. 3, p. 17.
18. Radtsig, V.A. and Kostritsa, S.N., *Kinet. Katal.*, 2000, vol. 41, no. 2, p. 267.
19. Bobyshev, A.A., Radtsig, V.A., and Senchenya, I.N., *Kinet. Katal.*, 1990, vol. 31, no. 4, p. 931.
20. Kazanskii, V.B., Gritskov, A.M., and Andreev, V.M., *Dokl. Akad. Nauk SSSR*, 1977, vol. 235, no. 1, p. 136.
21. Bobyshev, A.A. and Radtsig, V.A., *Kinet. Katal.*, 1990, vol. 31, no. 4, p. 925.
22. Atkinson, K., Baulch, D.L., Cox, R.A., *et al.*, *J. Phys. Chem. Ref. Data*, 1989, vol. 18, p. 881.
23. Radtsig, V.A. and Bobyshev, A.A., *Phys. Status. Solidi B*, 1986, vol. 133, p. 621.
24. Radtsig, V.A., *Kinet. Katal.*, 1979, vol. 20, no. 2, p. 456.
25. Morrow, B.A. and Cody, I.A., *J. Phys. Chem.*, 1976, vol. 80, no. 18, p. 1998.
26. Bunker, D.C., Haaland, D.M., Michalske, T.A., and Smith, W.L., *Surf. Sci.*, 1989, vol. 222, p. 95.